



Spatial distribution, structural characterization and weathering of tarmats along the west coast of Qatar



S. Veerasingam, Jassim A. Al-Khayat, K.P. Haseeba, V.M. Aboobacker, Shafeeq Hamza, P. Vethamony*

Environmental Science Center, Qatar University, P.O. Box: 2713, Doha, Qatar

ARTICLE INFO

Keywords:

Tarmat
Weathering
ATR-FTIR
Spectral indices
West coast of Qatar

ABSTRACT

Oil pollution resulting from natural and anthropogenic activities in the Arabian Gulf as well as oil residue in the form of tarmat (TM) deposited on the coast is a major environmental concern. The spatial distribution, chemical composition and weathering pattern of tarmat along the west coast of Qatar has been assessed based on the TM samples collected from 12 coastal regions. The range of TM distribution is 0–104 g m⁻¹ with an average value of 9.25 g m⁻¹. Though the current TM level is thirty-fold lesser than that was found during 1993–1997 (average 290 g m⁻¹), the distribution pattern is similar. The results of ATR-FTIR spectroscopy indicate that aromatic compounds are higher in the north (N) coast TMs than those found in the northwest (NW) and southwest (SW) coasts, and Carbonyl Index values indicate that TM of NW coast is highly weathered compared to those found in the N and SW coasts.

1. Introduction

Tarmat (TM) or oil residue is originated from natural and anthropogenic marine oil spills, and deposited as mats of different sizes and forms on the inter-tidal or coastal belt after going through various weathering processes. During the 1991 Gulf War, about 10.8 million barrels of crude oil was spilled (world's largest oil spill) along with a large amount of ash fall-out (Soliman et al., 2019). Other sources in the Arabian Gulf are spills during offshore oil exploration, oil tanker accidents, oil well blowouts, accidental and deliberate release of bilge and ballast water from ships, river run-off and discharges through municipal sewage and industrial effluents (Dashtbozorg et al., 2019). Two decades ago, Al-Madfa et al. (1999) quantified TM deposits along the Qatar coast and reported that north and northwest coasts of Qatar were severely affected by 1991 Gulf War oil spill. The oil residues from NW coast of Qatar subject to GC-MS and CHEMSIC source identification methods revealed that the residues were originated from two different sources, viz., Saudi Arabia and Kuwait crude oils (Al-Kaabi et al., 2017). Researchers have documented oil spill contaminants at various beaches located along the western and eastern coasts of Qatar (Dahab and Al-Madfa, 1993; Al-Madfa et al., 1999; Al-Kaabi et al., 2017; Rushdi et al., 2017; Soliman et al., 2019; Arekhi et al., 2020). In addition to previous oil spills, Qatar coast is continuously exposed to fresh oil spills, however, may not be in large quantities.

The hazardous or toxic substances of oil residues may have severe short or long-term impacts on marine ecosystems and economy, depending on weather condition, location and ecological sensitivity of the area around a spill (Carpenter, 2019). Even in the absence of acute toxicity, oil persistence in sediments can induce long-term ecological effects through complex biological interactions. The bioavailable oil fractions can cause chronic sub-acute toxicological effect (poor health, reduced growth and reproduction, low recruitment rates, etc.), which can alter population dynamics, disrupt trophic interactions and structure of natural communities within the ecosystems (Peterson et al., 2003; Bejarano and Michel, 2010). The origin and source oil of a particular TM can be determined by comparing the tar composition with that of suspected source oils, including a specific tanker, spill or natural seep – a method referred to as “fingerprinting” (Ehrhardt and Blumer, 1972; Van Vleet et al., 1984; Wang et al., 1998; Zakaria et al., 2001; Suneel et al., 2013, 2014). A number of analytical techniques (UV spectroscopy, GLC, TLC, Gas Chromatography coupled with MS, FID, IRMS, AES, and GC × GC and FT-ICR-MS) are employed to fingerprint and characterize the oil spills/residues in terms of age, degree of weathering, biodegradation and possible sources (Warnock et al., 2015).

The size, mobility or transport and location of TM deposit are influenced by its exposure to different types of weathering. For example, weathering is higher for the TM from the supratidal zone than the

* Corresponding author.

E-mail address: pvethamony@qu.edu.qa (P. Vethamony).

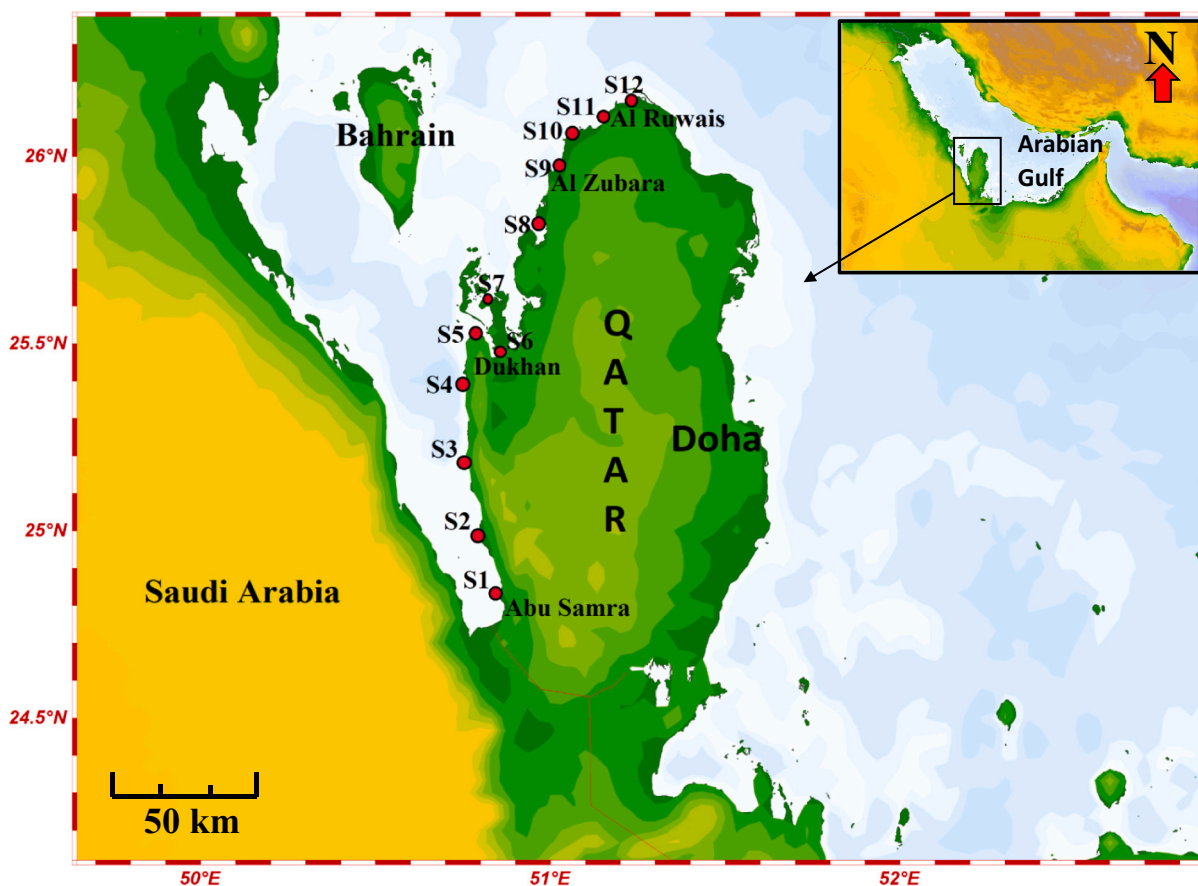


Fig. 1. The study area and sampling locations; S1 – Abu Samra, S2 – Umm Bab, S3 – Fahahil, S4 – Dukhan, S5 – Ras Al Ghariya, S6 – Zekreet, S7 – Al Buruq, S8 – West Island, S9 – Al Zubara, S10 – Al Arish, S11 – Abu Dhalouf, S12 – Al Ruwais.

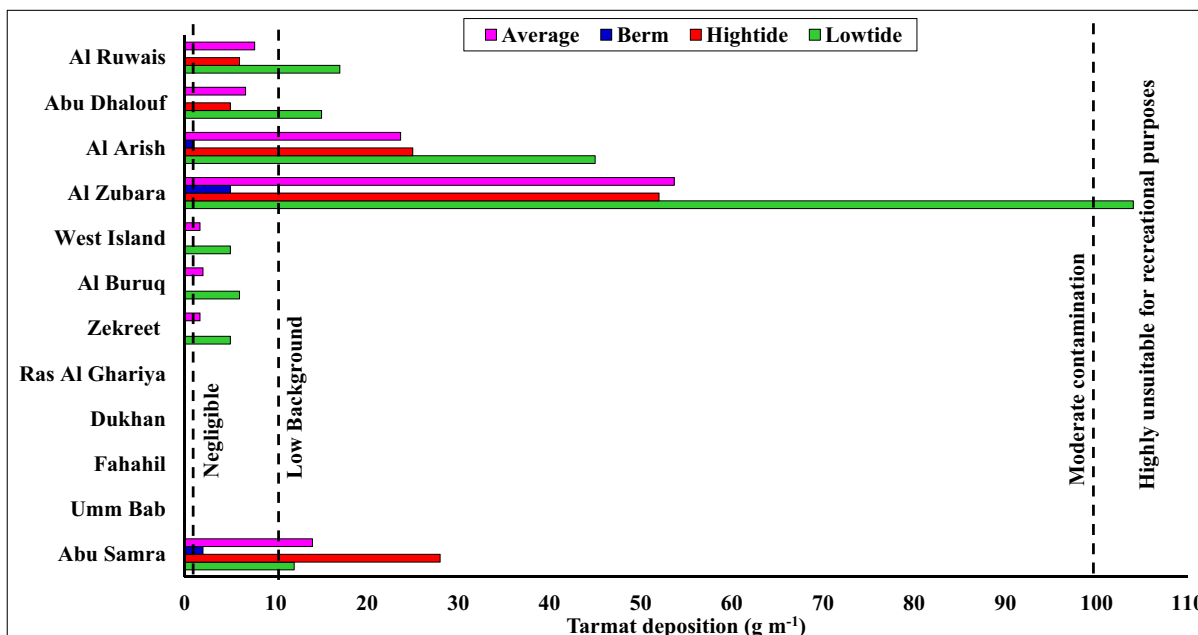


Fig. 2. Spatial distribution of tarmat deposition at 36 locations in 12 beaches along the west coast of Qatar.

submerged samples from the intertidal (Elango et al., 2014; White et al., 2016). Spreading and evaporation are the initial processes of oil weathering to start with, followed by dissolution, biodegradation, photo-oxidation, emulsification and sedimentation (Aeppli et al., 2012; Suneel et al., 2013; Warnock et al., 2015; Shirneshan et al., 2016;

Morrison et al., 2018), and therefore, properties of the spilled crude oil are altered significantly. The Fourier Transform Infrared (FTIR) Spectroscopy gives reliable information of chemical composition such as aliphatic and aromatic compounds, oxygenation rate and condensation degree of polyaromatic compounds (Permanyer et al., 2002; Chen et al.,

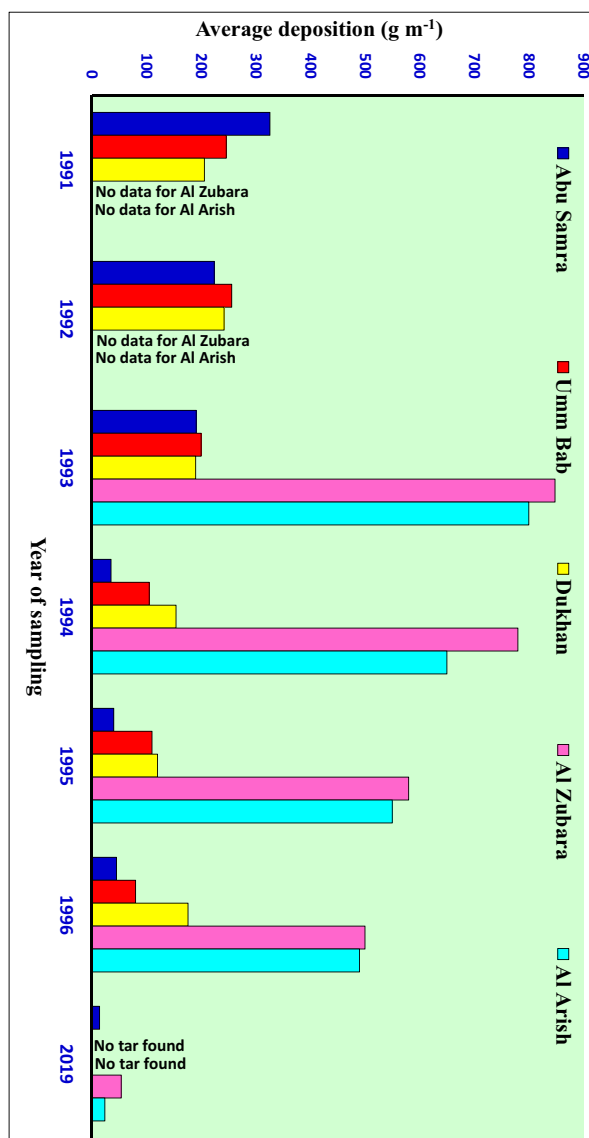


Fig. 3. Comparison of tar mat deposition along the west coast of Qatar (present study with Al-Madfa et al., 1999).

2015; Yang et al., 2019). Molecular level analysis of oil residues in the environment provides critical insight into changes in chemical composition of oil and the weathering processes responsible for these changes. Many researchers found that FTIR spectroscopy can be used as a rapid technique to characterize the chemical composition and weathering pattern (Permanyer et al., 2002; Abbas et al., 2006; White et al., 2016; Morrison et al., 2018).

Literature review reveals that the level of TM contamination along the Qatar coast due to Gulf war oil spill had been assessed only two decades ago. Since then the physical and chemical characteristics of stranded TM have been changed as a result of physical, chemical and biological processes. Hence, the present study is taken up with the following objectives: i) to assess the current status of TM contamination along the west coast of Qatar, ii) to characterize the structural and chemical composition of TM using ATR-FTIR Spectroscopy, iii) to examine the weathering pattern of TM using FTIR spectral indices and iv) to improve our understanding on the sources of TM on the Qatar coast.

2. Materials and methods

2.1. Study area

The Qatar peninsula covers an area of 11,651 km^2 , with a coastline running about 700 km, including a number of coastal islands from the Salwa Bay at the border of Saudi Arabia to the border of United Arab Emirates (Rushdi et al., 2017). The exclusive economic zone (EEZ) of Qatar encompasses approximately 35,000 km^2 with an average water depth of 35 m. In recent decades, Qatar has undergone rapid and intense urban renewal and development. The population of Qatar has increased from 0.025 million in 1950 to 2.83 million in 2019 (UN-DESA, 2019). Qatar coast is enriched with diverse ecosystems including mangrove forests, intertidal mudflats (sabkha), seagrass beds and coral reefs. These ecosystems contain a substantial proportion of Qatar's total biodiversity, and support an estimated 97% of US\$ 67 million annual commercial fisheries, the highest value resource sector after petroleum (Burt et al., 2017). The land area is largely flat and stony deserts. The range of mean daily air temperature in summer is 30–35 °C (can exceed 50 °C), whereas the mean annual temperature is only 25 °C (Cheng et al., 2017). Although summer is humid, the area is very arid with a

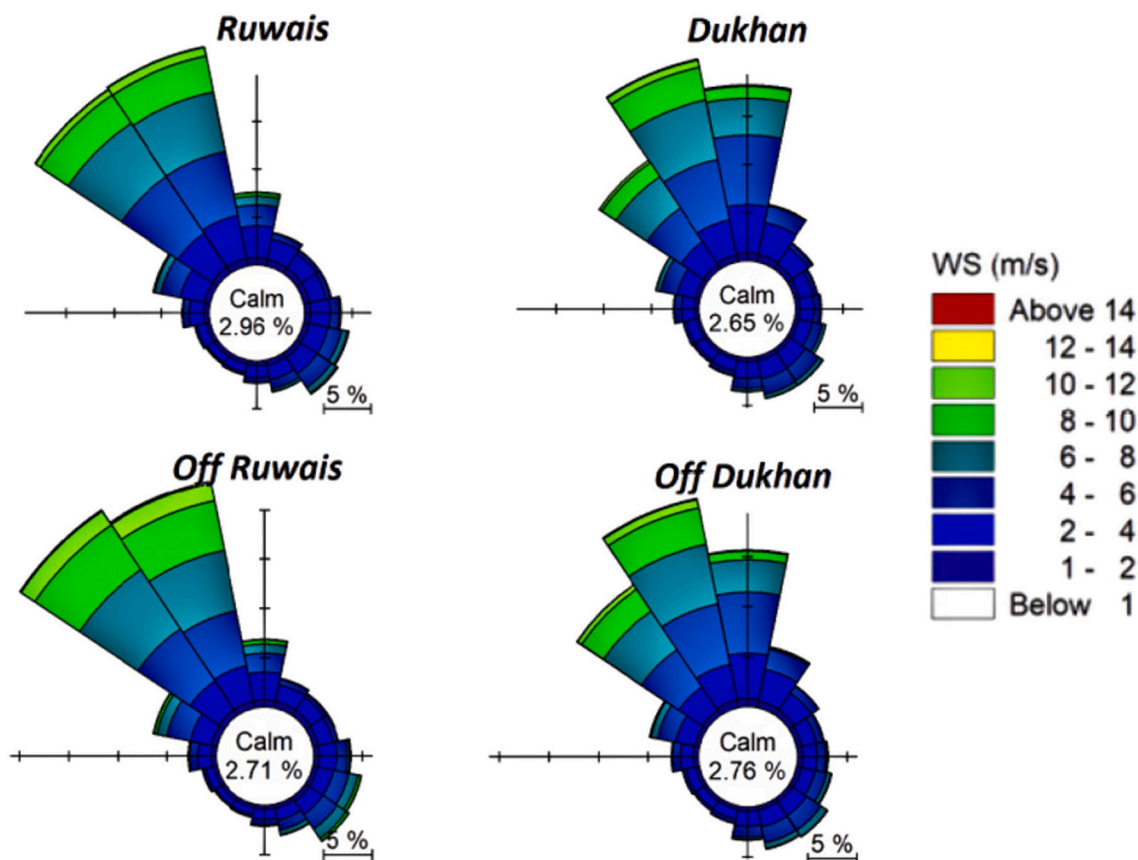


Fig. 4. Wind rose diagrams at select locations along the west coast of Qatar during 1979–2019 derived from ERA5.

mean annual rainfall of only 77 mm, and much of which occurs as rare high intensity events (Slowakiewicz et al., 2016). The wind regime is dominated by the NW to N regional shamal winds approaching Qatar mostly during early June to mid-July (summer shamal) and November to March (winter shamal), respectively (Yu et al., 2016; Sandeepan et al., 2018). These winds generate very high shamal swells, which can be traced even along the eastern Arabian Sea (Aboobacker et al., 2011).

2.2. Sampling

We have conducted TM sampling survey at 12 beaches from Abu Samra to Al Ruwais along the west coast of Qatar in September–November 2019 (Fig. 1). At each beach, three randomly selected transects (1 m wide) were marked in low tide, high tide and berm line (Fig. S1). TM samples within each transect were collected by metal spatula, and kept them in labelled aluminium foil bags. The collected samples were weighed in a high precision balance (0.1 mg).

2.3. Analytical methods

TM samples were analyzed using Attenuated Total Reflectance Fourier Transform Infrared (ATR-FTIR) spectroscopy (Thermo Scientific Nicolet iS10 spectrometer with Smart iTR Diamond crystal plate). Samples were sliced into half using a solvent-rinsed razor blade and a small internal section (~1 cm diameter) was removed and placed it on the ATR crystal for analysis. Absorbance spectra were recorded in the mid-infrared region (4000–600 cm^{-1}) using 32 scans at 2 cm^{-1} resolution. A background atmospheric spectrum was subtracted from all TM spectra. Peaks were integrated using Omnic software.

Different indices that represent the structural and functional features of TM were calculated on the basis of peak areas. Peak areas were measured from valley to valley (Permanyer et al., 2002). The following

indices were calculated to compare the structural and chemical composition of TMs using peak areas (Asemani and Rabbani, 2015):

Aliphatic index: $(A_{1460} + A_{1376}) / \Sigma A$, which represents all aliphatic compounds present in a sample.

Aromatic index: $A_{1600} / (A_{814} + A_{743} + A_{724})$, which represents all aromatic compounds present in a sample.

Carbonyl Index: $(A_{1700} / \Sigma A)$, which indicates the degree of photo-oxidation.

Long chain index: $A_{724} / (A_{1460} + A_{1376})$, which represents straight chain alkanes with 4 or more carbon atoms in a sample.

In the above indices, $\Sigma A = (A_{2953} + A_{2923} + A_{2862} + A_{1700} + A_{1600} + A_{1460} + A_{1376} + A_{1030} + A_{864} + A_{814} + A_{743} + A_{724})$. 'A' refers to the peak area in the absorption spectrum and the subscript number represents the wavenumber.

2.4. Current data

The CMEMS (Copernicus - Marine environment monitoring service) produces daily mean and monthly mean current velocities from their Operational Mercator global ocean analysis and forecast system covering the global ocean with 1/12° resolution (~9 km in the Indian Ocean) and has 50 vertical layers. It uses a global ocean model based on NEMO code v3.1; (Madec, 2012) in the ORCA12 configuration, forced by 3-hourly ECMWF (European Centre for Medium-Range Weather Forecast) operational winds and corresponding heat and freshwater fluxes. It captures all effects in driving the ocean currents, including the Ekman drift from the wind. A range of satellite and in-situ data are used to update and correct the simulated ocean state (Lellouche et al., 2013, 2018). In this study, we used monthly mean current velocities obtained from CMEMS to describe the circulation pattern during winter and

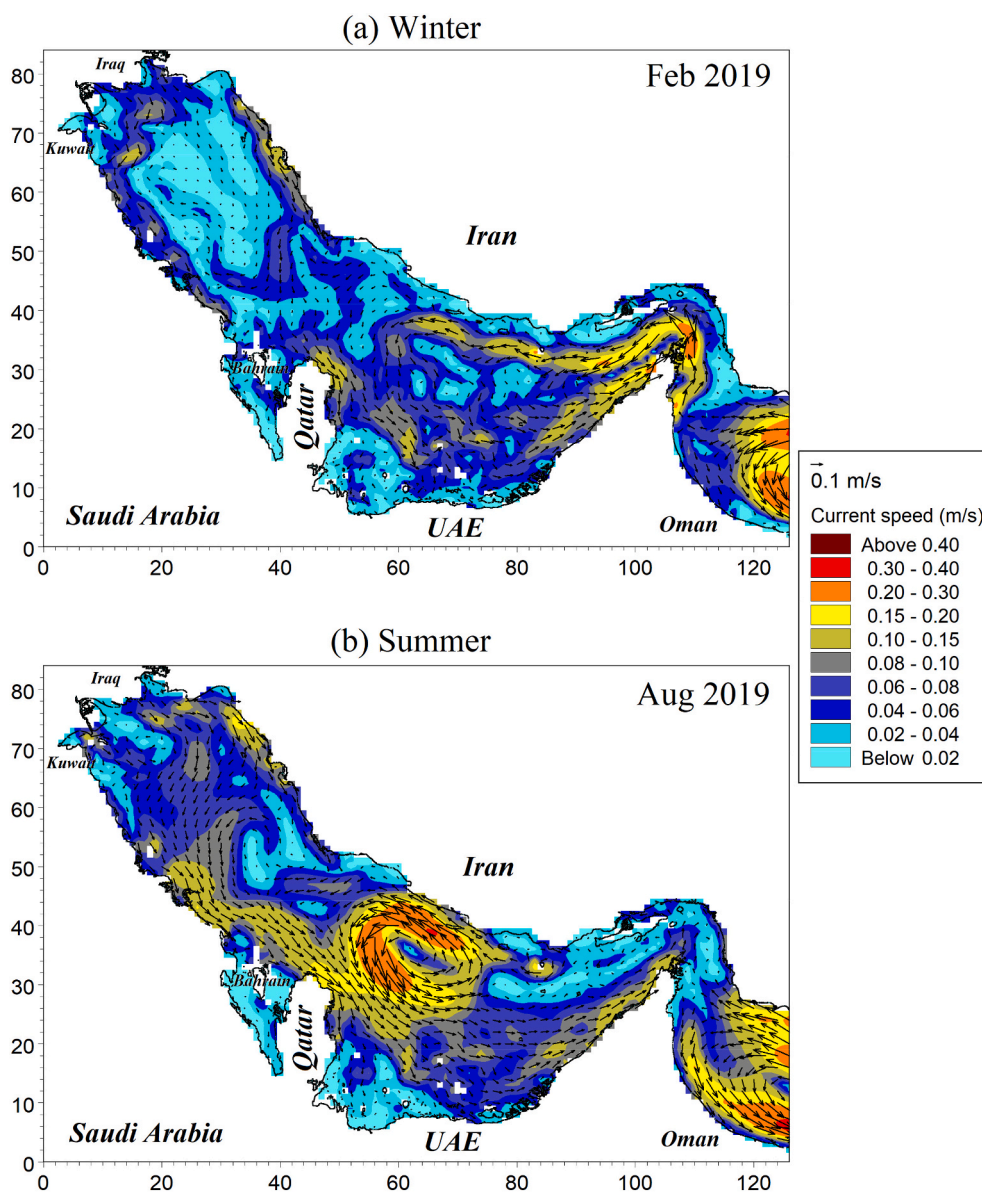


Fig. 5. The monthly mean current speeds and directions in the Arabian Gulf representing (a) Winter (Feb 2019) and (b) Summer (Aug 2019).

summer and their influence on the transport of oil in the Arabian Gulf.

3. Results and discussion

3.1. Physical characteristics and distribution of TM

The field campaigns clearly showed that the TM along the west coast of Qatar exhibit in several physical forms, wide range of sizes and with different degrees of weathering. The physical appearance of TM indicated that these were originated from relatively old spills, and none of the samples showed the indication of any fresh slicks. The surface of TM was highly weathered and looked like asphalt (Fig. S2). The distribution of TMs at 36 sampling locations (from the 12 beaches) along the west coast of Qatar is presented in Fig. 2. The spatial distribution shows considerable variability in TM quantity, ranging between ND (not detected) and 104 g m^{-1} with an average value of 9.25 g m^{-1} . The largest quantity of TM has been observed on the north and northwest coasts of Qatar. The southern beaches were less contaminated with TM. However, among the 12 beaches, no TM was found at 4 beaches on the central part of west coast of Qatar. The variability in the spatial

distribution of TM could be due to source of oil, speed and direction of winds, currents and degree of exposure/protection of the beach. Oil spills are carried away by surface winds and coastal circulation, and the regions of deposition depends on residual flow, coastal topography and coastal geomorphology. The residual flow in the Arabian Gulf could be attributed to two principal factors: (i) a net anticlockwise circulation generated by wind forcing coupled with Coriolis effects and (ii) effect of horizontal density gradients, generated and sustained by evaporative losses and radiative heat transfer, and to a lesser extent by freshwater inflow at the head of the Gulf (Lardner et al., 1988). Large quantities of oil are transported to south by northwest winds and regional circulation, affecting virtually most of the beaches along the Qatar coast (Al-Kaabi et al., 2017).

Corbin et al. (1993) classified the level of TM contamination based on their accumulation in the beach as follows: Negligible ($0\text{--}1 \text{ g m}^{-1}$), Low background ($1\text{--}10 \text{ g m}^{-1}$), Moderate ($10\text{--}100 \text{ g m}^{-1}$) and highly unsuitable for recreational activities ($> 100 \text{ g m}^{-1}$). The occurrence of TMs along the NW and N parts of Qatar indicate moderate level of petroleum contamination to severe contamination. The quantity of stranded TMs along the coast showed the following order: low tide >

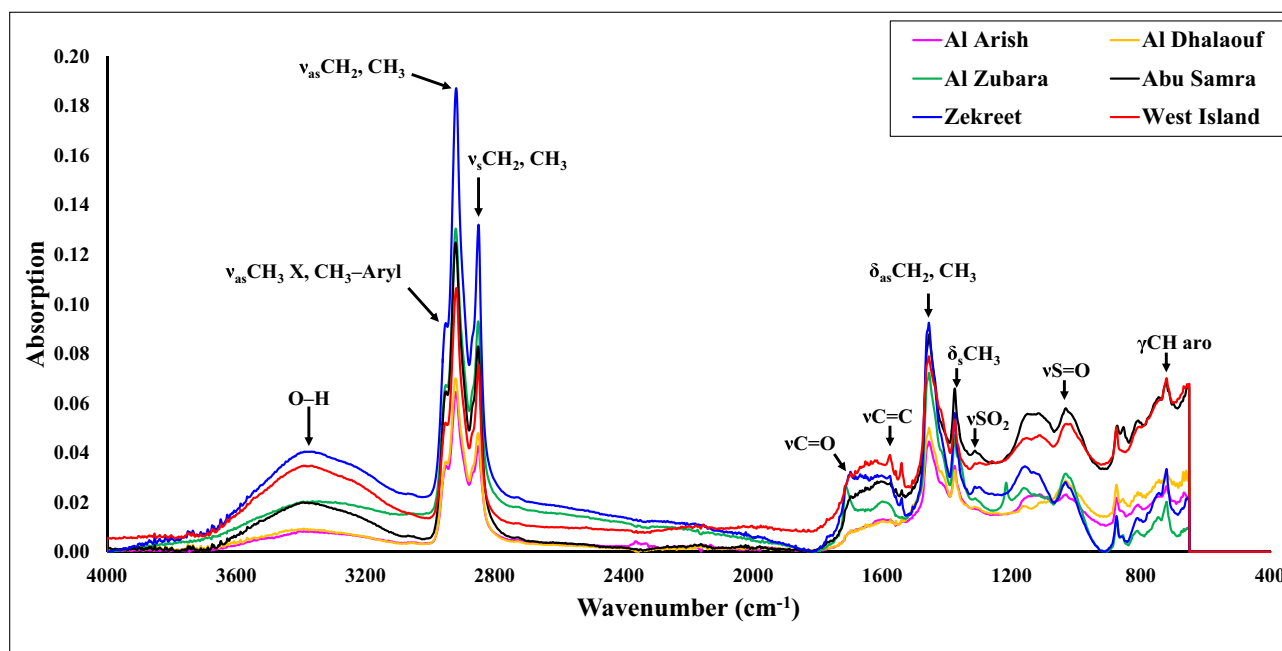


Fig. 6. Representative ATR-FTIR spectra of tarmat deposited along the west coast of Qatar.

Table 1

FTIR characteristic absorption peak assignments for tarmat samples.

| Characteristic peaks (cm ⁻¹) | Assignment | References |
|------------------------------------------|---------------------------------------------------------------------------------------------------------------------------------------------------------------------------------------|---------------------------------------------------------------------------------------------------------------------------------------------------------------------------------------------------------------------------------------------------|
| 3650–3200 | O–H stretching vibration | Permanyer et al. (2002), Fernandez-Varela et al. (2005), Lis et al. (2005), Abbas et al. (2006), Fresco-Rivera et al. (2007), Asemani and Rabbani (2015), White et al. (2016), Riley et al. (2016), Morrison et al. (2018) and Yang et al. (2019) |
| 3080–3010 | = C–H stretching vibration | |
| 2953 | C–H asymmetric stretching vibration in CH ₃ (ν _{as} CH ₃) and C–H stretching in alkanes | |
| 2923 | C–H asymmetric stretching vibration in CH ₂ (ν _{as} CH ₂) | |
| 2862 | C–H symmetric stretching vibration in CH ₃ (ν _s CH ₃) and C–H asymmetric stretching vibration in CH ₂ (ν _{as} CH ₂) | |
| 1700 | C=H stretching vibration | |
| 1600 | C=C stretching vibration aromatic compounds | |
| 1460 | Methyl C–H (CH ₂ and CH ₃) asymmetric/symmetric bending vibrations | |
| 1376 | C–H (CH ₃) symmetric bending vibrations | |
| 1030 | C–OH stretching vibrations | |
| 864, 814, 743 | Out of plane bending vibrations of C–H in aromatic compounds | |
| 724 | Out of plane bending vibrations of C–H in aromatic compounds and bending vibrations (rocking type) of C–H in CH ₂ | |

high tide > berm line. Comparison of the beached TMs with historical data (Al-Madfa et al., 1999) indicates that the present quantity (average 9.25 g m⁻¹) is thirty-fold lesser than those found during 1993 to 1997 (290 g m⁻¹). To our knowledge, there are no records accounting for the total amount of TMs removed from the Qatar coast since the time of Gulf War oil spill, though tarmats have been removed and dumped at some coastal regions (for example, near Al Jumail, NW coast of Qatar). However, as TMs are exposed to the environment, oil components have degraded over the time through physical, chemical and biological factors. Though the present data show a significant decline in the amount of TM compared to the historical data, the current deposition trend of TM is similar to the historical deposition pattern, i.e. northwestern part is still highly contaminated (Fig. 3).

3.2. Controlling factors for the transportation and distribution of tarmats/oil residues

It is known that the Arabian Gulf was heavily impacted by the Gulf

War oil spill in 1991. The spillage of crude oil during exploration, loading and transportation (tankers or pipelines) in the Arabian Gulf is recorded in the satellite data (Zhao et al., 2015; Evtushenko et al., 2018). The detailed nautical charts of marine traffic intensity and oil tanker routes show that navigation routes (especially tankers) are well connected to the major oil transportation bases and ports in the Arabian Gulf (Fig. S3). The historical wind data obtained from ERA5 (Hersbach et al., 2019) show that offshore winds blow predominantly in the northwesterly direction throughout the year over Qatar (Fig. 4). Wind and waves will dominate the surface drifting of floating particles through Ekman drift, windage and Stokes drift mechanisms (Zhang, 2017). The circulation pattern in the Arabian Gulf shows that the inflow current along the Iranian coast is weakened by the strong shamal winds in the winter, but in summer, it strengthens and extends almost to the head of the Gulf (Fig. 5).

A cyclonic circulation gyre sets in the southern Gulf is driven by the inflow of surface water from the Arabian Sea through the Strait of Hormuz. The run-off from Shatt Al-Arab in the northwest Gulf

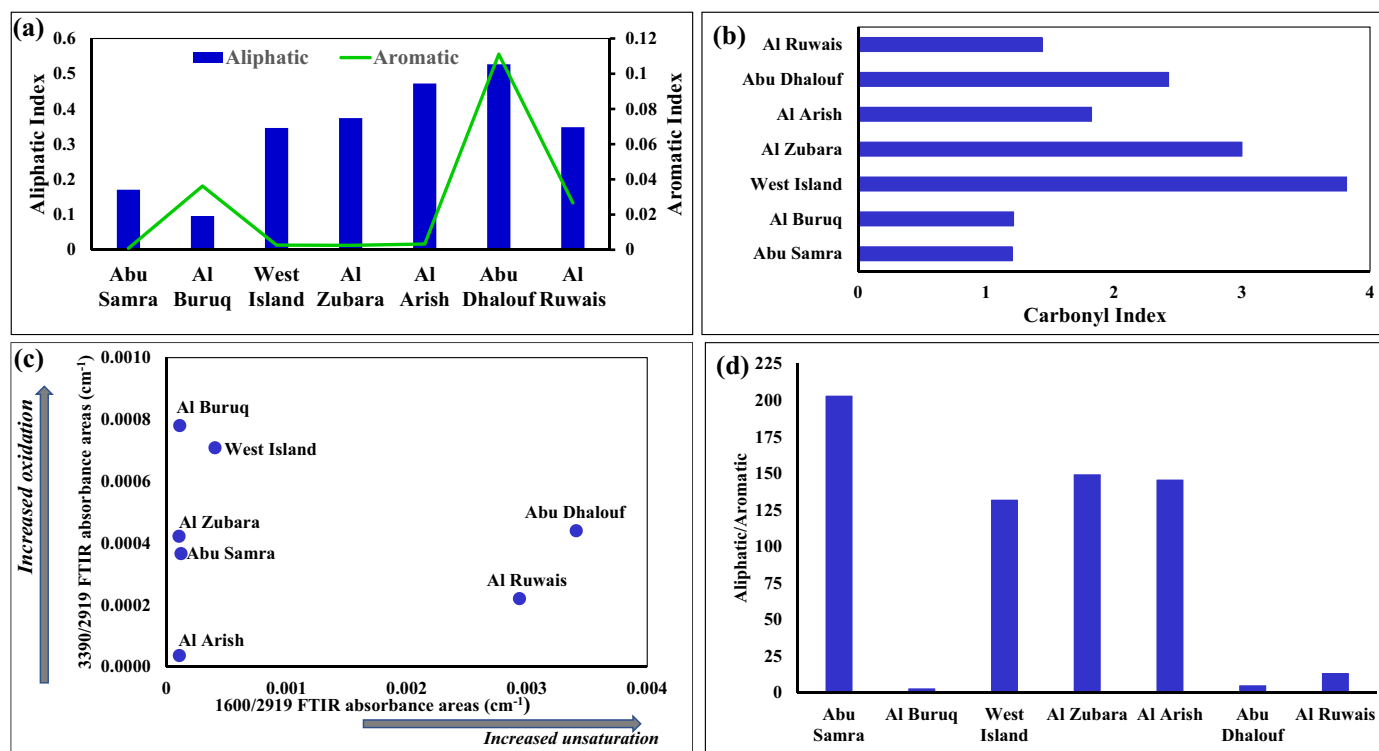


Fig. 7. (a) Aliphatic and aromatic indices of tarmats, (b) Carbonyl Index, (c) ratio of O–H vs C=C, where absorbance areas are normalized with C–H absorbance area and (d) Ratio of aliphatic compounds over aromatic compounds.

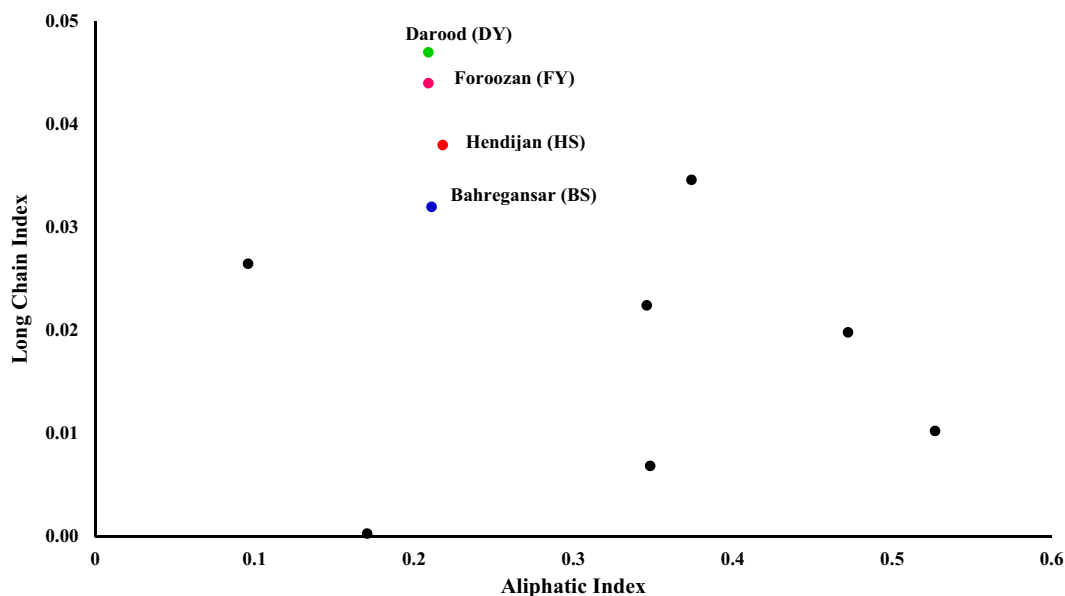


Fig. 8. The long chain index vs. aliphatic index of tarmats in Qatar (black dots) and crude oil asphaltene from four different Iranian oil fields.

maintains a cyclonic circulation, which otherwise would be an anti-cyclonic. A southward coastal jet exists between the head of the Gulf and east of Qatar depending on the winds (Reynolds, 1993). Moreover, the central part of the west coast of Qatar is in the shadow zone of Bahrain, and that might have relatively reduced the transport and accumulation of oil spill, tarballs or tarmats during Gulf War in the central coast, compared to the north. In addition to physical characteristics of oil (quantity, density and viscosity), dynamics of the water body due to winds, waves, tides and currents also important to control the transport and distribution of TMs along the west coast of Qatar, and this is also the reason for maximum TM accumulation along the northern coast

compared to the southern coast.

3.3. Chemical composition and structural characterization of TMs using ATR-FTIR

In ATR-FTIR spectroscopy, mid-infrared spectral region is the most commonly used infrared spectral region, which corresponds to the transition from ground state to the first excited state, and can be accompanied by the transition of rotational energy level (Zhang et al., 2019). Representative FTIR spectra for TM samples are shown in Fig. 6. These spectra were evaluated using different spectral ranges with

stretching, bending and rocking vibrations. The characteristic peaks for aliphatic hydrocarbons were observed at $3100\text{--}2800\text{ cm}^{-1}$, 1460 cm^{-1} , 1377 cm^{-1} and 720 cm^{-1} , respectively. Peaks at 1600 cm^{-1} and $900\text{--}700\text{ cm}^{-1}$ indicate the presence of aromatic hydrocarbons. The presence of oxygenated functional groups was observed at $1800\text{--}1600\text{ cm}^{-1}$ (Abbas et al., 2006; White et al., 2016; Zhang et al., 2019). The peak assignments for functional groups in the variety of TMs are presented in Table 1. The aromatic and aliphatic compounds are significant and fundamental structures in TM. Therefore, in order to compare the presence of these compounds among the collected TMs, the aliphatic and aromatic indices were calculated using ATR-FTIR data (Fig. 7a). The aliphatic and aromatic compounds are higher in the NW coast samples than in the samples of N and SW coasts of Qatar.

3.4. Weathering state of TMs

The extreme warm weather condition in Qatar leads to acceleration in the oil weathering processes, including physical removal, evaporation and biodegradation processes (Al-Kaabi et al., 2017). Therefore, Carbonyl Index (CI) was calculated for TMs from the FTIR spectra to study the photo-oxidation process (Fig. 7b). CI is a typical photo-oxidation indicator, which increases with weathering (Fresco-Rivera et al., 2007). The CI values for TMs collected from the NW coast of Qatar (West Island and Al Zubara) indicate that these TMs were highly weathered than those found in the N and SW coasts of Qatar. The large variation in weathering observed in the TMs of west coast of Qatar could be an indication that the source oil might be of different origin or might have been formed at a different timing. PAH analysis of oil residues and sediments from Qatar coast using GC-MS and CHEMSIC techniques showed that the crude oils were from at least two different sources, i.e., Saudi Arabia and Kuwait (Al-Kaabi et al., 2017).

The ratio between the Oxygen containing functional groups (O-H at 3390 cm^{-1}) and C=C absorbance (at 1600 cm^{-1}) of TMs (Fig. 7c) indicate that the increase in the relative proportion of aromatic compounds is likely to be due to the persistence of compounds that are relatively resistant to weathering such as alkylated chrysenes (White et al., 2016). Riley et al. (2016) used ATR-FTIR method to fingerprint the weathered and non-weathered Middle Eastern crude and heavy fuel oil asphaltenes. The spectrum for the weathered sample showed a higher absorbance in the regions ($650\text{--}930\text{ cm}^{-1}$) and ($1260\text{--}1520\text{ cm}^{-1}$) compared to the spectrum for non-weathered sample (an additional band structure around 880 cm^{-1}). The FTIR results of weathered TMs obtained from the present study also match very well with that of Riley et al. (2016). Earlier studies found that most of the heavily weathered TMs deposited along the Qatar coast (Al-Madfa et al., 1999; Al-Kaabi et al., 2017) and the PAHs present in the sediments (Rushdi et al., 2017; Soliman et al., 2019) were originated from the Gulf War. Most of the collected TMs showed heavily weathered solid surface outside, and relatively non-weathered oil interior, indicating that degradation of oil is a very slow process (Al-Kaabi et al., 2017).

3.5. Maturity degree of tarmats

Chemical processes changing the macromolecular structure of oil during thermal maturation are evident with increasing maturity as FTIR spectroscopic shifts (Lis et al., 2005). Abbas et al. (2012) found that the relative abundance of saturated and aromatic hydrocarbons could be considered as maturity indicators influencing directly the quality of oils. Therefore, the ratio of aliphatic compounds over aromatic compounds was used in the present study to evaluate the maturity degree of TMs (Peters and Moldowan, 1993). Higher the ratio, higher is the maturity degree of the oils (Permanyer et al., 2002). With increasing maturity, FTIR spectra show three trends: (i) decrease in the absorption of aromatic peaks, (ii) an increase in the aliphatic peaks and (iii) a loss

of oxygenated groups (carbonyl groups). In the aliphatic stretching region ($2800\text{--}3000\text{ cm}^{-1}$), the ratio between CH_2 and CH_3 could be identified. Lis et al. (2005) quantitatively related FTIR changes to increasing maturity, relying on vitrinite reflectance as the traditional and most commonly used proxy for thermal maturity in rocks containing organic matter. The calculated aliphatic to aromatic ratios of TMs clearly indicate that the samples from Abu Samra and NW coast of Qatar were more matured than those found along the north coast of Qatar (Fig. 7d).

3.6. Comparison of ATR-FTIR spectra of TMs with Iranian crude oil asphaltenes

The ATR-FTIR spectra of TMs collected from the west coast of Qatar show the same features with the KBr pellet technique FTIR analysis of four crude oil asphaltenes from different Iranian oil fields in the Arabian/Persian Gulf (Asemani and Rabbani, 2015). Though it is not possible to compare the changes in FTIR spectra of TMs (measured by ATR-FTIR) with crude oil asphaltenes (measured by FTIR with KBr pellet technique), several peaks including O-H, C-H, C=O, C=C and C-OH exhibit good agreement between these two methods. It is evident from the cross plot of aliphatic index vs. long chain index of TMs collected along the west coast of Qatar and Iranian crude oil asphaltenes (Fig. 8) that the ATR-FTIR spectra of TMs and Iranian crude oil asphaltenes are comparable in terms of peaks that were observed and measured. From the results of analyses and discussion, it is possible to state that the ATR-FTIR method is a rapid approach to characterize and study the weathering of TMs without any tedious sample preparation or solvent extraction.

4. Conclusions

The spatial distribution, chemical composition and weathering pattern of TMs along the west coast of Qatar have been investigated. The NW coast of Qatar is highly contaminated with tarmats, and the current status of contamination shows that it is thirty-fold lesser than those found during Gulf War oil spill. The prevailing winds and currents might have dominated the surface drifting of floating oil residues towards the NW coast of Qatar. Chemical and structural properties of TMs were calculated using FTIR spectral indices (i.e., aliphatic, aromatic, long chain and carbonyl indices) and some of their features are comparable to that of Iranian crude oil asphaltenes. The aromatic compounds of TMs are lesser in the NW coast than those found in the northern coast. Carbonyl Index values indicate that TM samples from the NW coast are highly weathered than those found in the north and SW coasts. The concentration of hydrocarbons (including aliphatic and aromatic) in TM can be used to study the ecological risks on sediment associated biota. The quantification of the concentration of PAHs in large number of samples using GCMS and other chemical analyses are very expensive and time consuming, and for such analyses, ATR-FTIR method could be used to characterize the oil residues and study their weathering patterns.

CRediT authorship contribution statement

S. Veerasingam: Conceptualization, Methodology, Investigation, Writing - original draft, Writing - review & editing. **Jassim A. Al-Khayat:** Methodology, Investigation, Writing - review & editing. **K.P. Haseeba:** FTIR analysis. **V.M. Aboobacker:** Methodology, Investigation, Writing - review & editing. **Shafeeq Hamza:** Methodology, Investigation. **P. Vethamony:** Conceptualization, Investigation, Writing - original draft, Writing - review & editing, Supervision, Funding acquisition.

Declaration of competing interest

The authors declare that they have no known competing financial interests or personal relationships that could have appeared to influence the work reported in this paper.

Acknowledgement

We thank Prof. Hamad Al-Saad Al-Kuwari, Director, Environmental Science Center, Qatar University (QU) for his constant encouragement and support. We acknowledge Gas Processing Center, QU, where ATR-FTIR analysis was performed. We acknowledge ORS, QU for awarding the Project (QUEX-ESC-QP-TM-18/19), funded by the Qatar Petroleum.

Appendix A. Supplementary data

Supplementary data to this article can be found online at <https://doi.org/10.1016/j.marpolbul.2020.111486>.

References

- Abbas, O., Dupuy, N., Rebufa, C., Vrielynck, L., Kister, J., Permanyer, A., 2006. Prediction of source rock origin by chemometric analysis of Fourier transform infrared-attenuated total reflectance spectra of oil petroleum: evaluation of aliphatic and aromatic fractions by self-modeling mixture analysis. *Appl. Spectrosc.* 60, 304–314.
- Abbas, O., Rebufa, C., Dupuy, N., Permanyer, A., Kister, J., 2012. PLS regression on spectroscopic data for the prediction of crude oil quality: API gravity and aliphatic/aromatic ratio. *Fuel* 98, 5–14.
- Aboobacker, V.M., Vethamony, P., Rashmi, R., 2011. "Shamal" swells in the Arabian Sea and their influence along the west coast of India. *Geophys. Res. Lett.* 38 (3), L03608.
- Aeppli, C., Carmichael, C.A., Nelson, R.K., Lemkau, K.L., Graham, W.M., Redmond, M.C., Valentine, D.L., Reddy, C.M., 2012. Oil weathering after the Deepwater Horizon disaster led to the formation of oxygenated residues. *Environ. Sci. Technol.* 46, 8799–8807.
- Al-Kaabi, N.S., Kristensen, M., Zouari, N., Solling, T.I., Bach, S.S., Al-Ghouthi, M., Christensen, J.H., 2017. Source identification of beached oil at Al Zubarah, Northwestern Qatar. *J. Pet. Sci. Eng.* 149, 107–113.
- Al-Madfa, H., Abdel-Moati, M.A.R., Al-Naama, A., 1999. Beach tar contamination on the Qatari coastline of the Gulf. *Environ. Int.* 25, 505–513.
- Arkhi, M., Terry, L.G., John, G.F., Al-Khayat, J.A., Castillo, A.B., Vethamony, P., Clement, T.P., 2020. Field and laboratory investigation of tarmat deposits found on Ras Rakan Island and northern beaches of Qatar. *Sci. Total Environ.* 735, 139516.
- Asemani, M., Rabbani, A.R., 2015. Oil-oil correlation by FTIR spectroscopy of asphaltene samples. *Geosci. J.* 20, 273–283.
- Bejarano, A.C., Michel, J., 2010. Large-scale risk assessment of polycyclic aromatic hydrocarbons in shoreline sediments from Saudi Arabia: environmental legacy after twelve years of the Gulf war oil spill. *Environ. Pollut.* 158, 1561–1569.
- Burt, J.A., Ben-Hamadou, R., Abdel-Moati, M.A.R., Fanning, L., Kaitibie, S., Al-Jamali, F., Range, P., Saeed, S., Warren, C.S., 2017. Improving management of future coastal development in Qatar through ecosystem-based management approaches. *Ocean & Coastal Management* 148, 171–181.
- Carpenter, A., 2019. Oil pollution in the North Sea: the impact of governance measures on oil pollution over several decades. *Hydrobiologia* 845, 109–127.
- Chen, Y., Zou, C., Mastalerz, M., Hu, S., Gasaway, C., Tao, X., 2015. Applications of micro-Fourier transform infrared spectroscopy (FTIR) in the geological sciences – a review. *Int. J. Mol. Sci.* 16, 30223–30250.
- Cheng, W.L., Saleem, A., Sadr, R., 2017. Recent warming trend in the coastal region of Qatar. *Theor. Appl. Climatol.* 128, 193–205.
- Corbin, C.J., Singh, J.G., Ibiebele, D.D., 1993. Tar ball survey of six eastern Caribbean countries. *Mar. Pollut. Bull.* 26, 482–486.
- Dahab, O.A., Al-Madfa, H., 1993. Oil pollution in Qatari coastal sediments. *Environ. Pollut.* 81, 113–116.
- Dashtbozorg, M., Bakhtiari, A.R., Shushizadeh, M.R., Taghavi, L., 2019. Quantitative evaluation of n-alkanes, PAHs, and petroleum biomarker accumulation in beach-stranded tar balls and coastal surface sediments in the Bushehr Province, Persian Gulf (Iran). *Mar. Pollut. Bull.* 146, 801–815.
- Ehrhardt, M., Blumer, M., 1972. The source identification of marine hydrocarbons by gas chromatography. *Environ. Pollut.* 3, 179–194.
- Elango, V., Urbano, M., Lemelle, K.R., Pardue, J.H., 2014. Biodegradation of MC252 oil in oil:sand aggregates in a coastal headland beach environment. *Front. Microbiol.* 5, 161.
- Evtushenko, N., Ivanov, A., Evtushenko, V., 2018. Oil pollution in the Persian Gulf: satellite-monitoring results in 2017. In: El-Askary, H., Lee, S., Heggy, E., Pradhan, B. (Eds.), *Advances in Remote Sensing and Geo Informatics Applications*. CAJG 2018. *Advances in Science, Technology & Innovation (IEREK Interdisciplinary Series for Sustainable Development)*. Springer, Cham.
- Fernandez-Varela, R., Suarez-Rodriguez, D., Gomez-Carracedo, M.P., Andrade, J.M., Fernandez, E., Muniategui, S., Prada, D., 2005. Screening the origin and weathering of oil slicks by attenuated total reflectance mid-IR spectrometry. *Talanta* 68, 116–125.
- Fresco-Rivera, P., Fernandez-Varela, R., Gomez-Carracedo, M.P., Ramirez-Villalobos, F., Prada, D., Muniategui, S., Andrade, J.M., 2007. Development of a fast analytical tool to identify oil spillages employing infrared spectral indexes and pattern recognition techniques. *Talanta* 74, 163–175.
- Hersbach, H., Bell, B., Berrisford, P., et al., 2019. Global reanalysis: goodbye ERA-Interim, hello ERA5. *ECMWF Newsletter* 159, 17–24.
- Lardner, R.W., Lehr, W.J., Fraga, R.J., Sarhan, M.A., 1988. A model of residual currents and pollutant transport in the Arabian Gulf. *Appl. Math. Modelling* 12, 379–390.
- Lellouche, J.M., Le Galloudec, O., Drévilon, M., Régnier, C., Greiner, E., Garric, G., Ferry, N., Desportes, C., Testut, C.E., Bricaud, C., Bourdalle-Badie, R., Tranchant, B., Benkiran, M., Drillet, Y., Daudin, A., Nicola, C.D., 2013. Evaluation of global monitoring and forecasting systems at Mercator Océan. *Ocean Sci.* 9, 57–81.
- Lellouche, J.M., Greiner, E., Le Galloudec, O., Garric, G., Regnier, C., Drevillon, M., Gasparin, F., Hernandez, O., Levier, B., Remy, E., Traon, P.-Y.L., 2018. Recent updates on the Copernicus Marine Service global ocean monitoring and forecasting realtime 1/12° high resolution system. *Ocean Sci. Discuss.* 14, 1093–1126.
- Lis, G.P., Mastalerz, M., Schimmelmann, A., Lewan, M.D., Stankiewicz, B.A., 2005. FTIR absorption indices for thermal maturity in comparison with vitrinite reflectance R0 in type-II kerogens from Devonian black shales. *Org. Geochem.* 36, 1533–1552.
- Madec, G., 2012. NEMO ocean engine. *Note du Pôle modélisation*. Inst Pierre-Simon Laplace, pp. 357.
- Morrison, A.E., Dhoonmoon, C., White, H.K., 2018. Chemical characterization of natural and anthropogenic-derived oil residues on Gulf of Mexico beaches. *Mar. Pollut. Bull.* 137, 501–508.
- Permanyer, A., Douifi, L., Lahcini, A., Lamontagne, J., Kister, J., 2002. FTIR and SUVF spectroscopy applied to reservoir compartmentalization: a comparative study with gas chromatography fingerprints results. *Fuel* 81, 861–866.
- Peters, K.E., Moldowan, J.M., 1993. *The Biomarker Guide, Interpreting Molecular Fossils in Petroleum and Ancient Sediments*. Prentice Hall, Englewood cliffs, NJ (363p).
- Peterson, C.H., Rice, S.D., Short, J.W., Esler, D., Bodkin, J.L., Ballachey, B.E., Irons, D.B., 2003. Long-term ecosystem response to the Exxon Valdez oil spill. *Science* 302, 2082–2086.
- Reynolds, R.M., 1993. Physical oceanography of the Gulf, Strait of Hormuz, and the Gulf of Oman – results from the *Mt Mitchell* Expedition. *Mar. Pollut. Bull.* 27, 35–59.
- Riley, B.J., Lennard, C., Fuller, S., Spikmans, V., 2016. An FTIR method for the analysis of crude and heavy fuel oil asphaltenes to assist in oil fingerprinting. *Forensic Sci. Int.* 266, 555–564.
- Rushdi, A.I., Al-Shaikh, I., El-Mubarak, A.H., Alnaimi, H.A.J.A., Al-Shamary, N., Hassan, H.M., Assali, M.A., 2017. Characteristics and sources of anthropogenic and biogenic hydrocarbons in sediments from the coast of Qatar. *Mar. Pollut. Bull.* 124, 56–66.
- Sandeepan, B.S., Panchang, V.G., Nayak, S., Krishnakumar, K., Kaihatu, J.M., 2018. Performance of the WRF model for surface wind prediction around Qatar. *J. Atmos. Ocean. Technol.* 35, 575–592.
- Shirneshan, G., Bakhtiari, A.R., Memariani, M., 2016. Identification of sources of tar balls deposited along the Southwest Caspian coast, Iran using fingerprinting techniques. *Sci. Total Environ.* 568, 979–989.
- Slowkiewicz, M., Whitaker, F., Thomas, L., Tucker, M.E., Zheng, Y., Gedl, P., Pancost, R.D., 2016. Biogeochemistry of intertidal microbial mats from Qatar: new insights from organic matter characterization. *Org. Geochem.* 102, 14–29.
- Soliman, Y.S., Alansari, E.M.A., Sericano, J.L., Wade, T.L., 2019. Spatio-temporal distribution and sources identifications of polycyclic aromatic hydrocarbons and their alkyl homolog in surface sediments in the central Arabian Gulf. *Sci. Total Environ.* 658, 787–797.
- Suneel, V., Vethamony, P., Zakaria, M.P., Naik, B.G., Prasad, K.V.S.R., 2013. Identification of sources of tar balls deposited along the Goa coast, India, using fingerprinting techniques. *Mar. Pollut. Bull.* 70, 81–89.
- Suneel, V., Vethamony, P., Naik, B.G., Kumar, K.V., Sreenu, L., Samiksha, S.V., Tai, Y., Sudheesh, K., 2014. Source investigation of the tar balls deposited along the Gujarat coast, India, using chemical fingerprinting and transport modelling techniques. *Environ. Sci. Technol.* 48, 11343–11351.
- UN-DESA, 2019. *United Nations Department of Economic and Social Affairs population dynamics*. <https://population.un.org/wpp/>.
- Van Vleet, E.S., Sackett, W.M., Reinhardt, S.B., Mangini, M., 1984. Distribution, sources and fates of floating oil residues in the Eastern Gulf of Mexico. *Mar. Pollut. Bull.* 15, 106–110.
- Wang, Z.D., Fingas, M., Landriault, M., Sigouin, L., Castle, B., Hostetter, D., Zhang, D.C., Spencer, B., 1998. Identification and linkage of tarballs from the coasts of Vancouver island and northern California using GC/MS and isotopic techniques. *J. High Resolut. Chromatogr.* 21, 383–395.
- Warnock, A.M., Hagen, S.C., Passeri, D.L., 2015. Marine tar residues: a review. *Water Air and Soil Pollution* 226, 68.
- White, H.K., Wang, C.H., Williams, P.I., Findley, D.M., Thurston, A.M., Simister, R.L., Aeppli, C., Nelson, R.K., Reddy, C.M., 2016. Long-term weathering and continued oxidation of oil residues from the Deepwater Horizon spill. *Mar. Pollut. Bull.* 113, 380–386.
- Yang, M., Cao, Z., Zhang, Y., Wu, H., 2019. Deciphering the biodegradation of petroleum hydrocarbons using FTIR spectroscopy: application to a contaminated site. *Water Sci.*

- Technol. 80, 1315–1325.
- Yu, Y., Notaro, M., Kalashnikova, O.V., Garay, M.J., 2016. Climatology of summer Shamal wind in the Middle East. *Journal of Geophysical Research Atmosphere* 121, 289–305.
- Zakaria, M.P., Okuda, T., Takada, H., 2001. Polycyclic aromatic hydrocarbon (PAHs) and hopanes in stranded tar balls on the coasts of Peninsular Malaysia: applications of biomarkers for identifying sources of oil pollution. *Mar. Pollut. Bull.* 42, 1357–1366.
- Zhang, H., 2017. Transport of microplastics in coastal seas. *Estuarine coastal and shelf science* 199, 74–86.
- Zhang, L., Huang, X., Fan, X., He, W., Yang, C., Wang, C., 2019. Rapid fingerprinting technology of heavy oil spill by mid-infrared spectroscopy. *Environ. Technol.* <https://doi.org/10.1080/09593330.2019.1626913>.
- Zhao, J., Temimi, M., Al Azhar, M., Ghedira, H., 2015. Satellite-based tracking of oil pollution in the Arabian Gulf and the sea of Oman. *Can. J. Remote. Sens.* 41, 113–125.